Transport properties and spin correlations of $La_{1.85-x}Sr_{0.15+x}Cu_{1-x}Fe_xO_4$

G. J. Xu*
Structure Research Laboratory and Department of Physics, University of Science and Technology of China, Hefei, Anhui 230026, People's Republic of China
and Materials Research Department, Risø National Laboratory, 4000 Roskilde, Denmark

Q. R. Pu, B. Liu, R. H. Tao, G. S. Wang, and Z. J. Ding
Structure Research Laboratory and Department of Physics, University of Science and Technology of China, Hefei, Anhui 230026, People's Republic of China

J.-C. Grivel and N. H. Andersen
Materials Research Department, Risø National Laboratory, 4000 Roskilde, Denmark
(Received 28 July 2003; revised manuscript received 9 October 2003; published 16 March 2004)

A series of double-doped $La_{1.85-x}Sr_{0.15+x}Cu_{1-x}Fe_xO_4$ ($0 \leqslant x \leqslant 1$) ceramic samples were prepared by the solid-state reaction method. The structure, transport properties, and spin correlations were studied by means of x-ray diffraction, resistivity, thermoelectric power (TEP) and electron spin resonance (ESR). Double doping causes an increase of the lattice parameter a and a decrease of c. A great discrepancy of the thermal activation energy is derived from the resistivity and TEP at high doping levels, which can be understood in terms of a polaron model. The ESR result indicates that the double doping influences the spin correlation of the CuO_2 plane markedly, which suggests that the Fe^{3+} spins change from localization to delocalization as x increases from low doping to high doping. A close relation between localized spin scattering and the broad peak in the TEP versus T curve is proposed. A comparison of the transport mechanism between the Fe doped and the Co and Ni doped La214 systems is given in this paper.

DOI: 10.1103/PhysRevB.69.104506 PACS number(s): 74.25.Fy, 74.72.Dn

INTRODUCTION

Extensive investigations have demonstrated that the normal state (NS) transport properties of high-T_c cuprates are unusual, and systematical studies of them are essential to understand the basic mechanism responsible for superconductivity. Elemental doping offers an important way towards this goal. One knows that conventional superconductors are very sensitive to magnetic element doping, and a little amount of magnetic doping can suppress superconductivity completely, while cuprate superconductors seem to be less sensitive to magnetic doping at non-CuO_2 planes. For substitution in the CuO_2 plane, both magnetic and nonmagnetic ions can destroy superconductivity with a few percent dopant concentration. Xiao *et al.*[1] have shown that the suppression of superconductivity by magnetic doping originates from magnetic pair-break effects. Ishikawa *et al.* have demonstrated that doping with magnetic ions, such as Co^{3+}, enhances the nearest-neighbor spin correlation, while nonmagnetic ions (Ga^{3+},Zn^{2+}) decrease the spin correlation energy.[2] These results clearly indicate that magnetic and nonmagnetic element doping into the CuO_2 plane have different influence on the NS properties.

Researchers believe that short range two-dimensional (2D) antiferromagnetic spin correlations play an important role in determining the anomalous characteristic of the transport properties. La_2CuO_4 (La214) is a charge-transfer insulator with long-range three-dimensional (3D) antiferromagnetic (AF) ordering.[3] Upon doping the long-range 3D AF ordering collapses dramatically, while the AF correlations within the CuO_2 plane persist well into the superconducting phase. Previously, there have been many reports on studies of the $La_{1.85}Sr_{0.15}Cu_{1-x}A_xO_4$ (A=Cr, Mn, Fe, Co, Ni, Zn, Ga, Al, Mg) systems.[1,4–11] Doping with Fe^{3+} shows the strongest T_c-suppression among the element dopings: T_c goes to zero at an Fe content x of only 1.8 at. %.[1] Marta Z. Cieplak and co-workers studied the spin dynamics of Fe doped La214,[12] but this work was limited to low doping levels ($x \leqslant 0.1$). To clarify the effect of doping on the NS transport properties, systematic investigations of Co and Ni doped La214 systems within the whole doping level ($0 \leqslant x \leqslant 1.0$) have been made and interesting results were obtained.[6,13] Fe is an important member of the transition metals and it possesses the largest moment of the transition elements in the La214 system. A study of its doping effect covering the full doping range is therefore important. In this study we direct our attention to the effect of Fe doping on the transport properties and spin correlation at high doping levels in the La214 system.

Since the rapid decrease of carrier concentration induced by Fe doping would limit the doping level, we have used double doping with Sr^{2+} and Fe^{3+} substitution for La^{3+} and Cu^{2+}, respectively, to keep the carrier concentration approximately constant. This also favors a study of the changes of the transport properties and spin correlation characteristics with doping. A systematic comparison of the transport mechanism between the Fe doped and the Co and Ni doped La214 systems is made.

EXPERIMENTAL METHOD

A series of polycrystalline samples of $La_{1.85-x}Sr_{0.15+x}Cu_{1-x}Fe_xO_4$ ($0 \leqslant x \leqslant 1.0$) were prepared using the standard solid-state reaction method. The detailed

TABLE I. Lattice parameters a, c, c/a, and unit-cell volume V of $La_{1.85-x}Sr_{0.15+x}Cu_{1-x}Fe_xO_4$ $(0 \leqslant x \leqslant 1)$.

Fe content x	a (Å)	c (Å)	c/a	V(Å^3)
$x=0$	3.7715	13.2132	3.5034	187.945
$x=0.1$	3.7831	13.1711	3.4814	188.477
$x=0.2$	3.7894	13.1719	3.4760	189.145
$x=0.3$	3.7979	13.1094	3.4517	189.093
$x=0.4$	3.8131	13.0532	3.4233	189.785
$x=0.5$	3.8251	13.0191	3.4001	190.481
$x=0.6$	3.8329	12.9465	3.3673	190.510
$x=0.8$	3.8535	12.8461	3.3336	190.762
$x=1$	3.8596	12.7500	3.3035	189.929

synthesis procedure has been reported previously.[14] The phase purity and the structure of the samples were studied by x-ray diffraction (XRD). The lattice parameters were determined from the d-values of the XRD peaks by a standard least-squares refinement method. A iodometric titration method was used to check the oxygen content of the samples within an error of 0.01. The resistivity as a function of temperature was measured using a standard four-probe method in a closed-cycle helium cryostat. The thermoelectric power (TEP, S) of the samples was measured by a differential method. The temperature difference between the two ends of the sample was controlled automatically to be 2 K with a precision of ± 0.01 K. The emf of the samples was measured using a Keithley 181 nanovoltmeter. The characteristic emf values are 20–120 μV and the accuracy of the voltmeter is better than 0.2 μV. The electron spin resonance (ESR) experiments were carried out at 100 K by a Bruker (ER-200D-SRC) reflection x-band-type spectrometer. The resonance frequency and magnetic field were measured using a frequency counter and a proton nuclear magnetic resonance (NMR) gaussmeter, respectively.

RESULTS AND DISCUSSION

The XRD patterns show that all the samples are single phase except for the $x=1.0$ sample which has some minor amount of impurity phases. The iodometric titration results show that except for the $x=1.0$ sample, the formula $La_{1.85-x}Sr_{0.15+x}Cu_{1-x}Fe_xO_{4\pm0.02}$ is suitable for all the other samples. For the $x=1.0$ sample the oxygen content is 3.94. Table I gives the lattice parameters a, c, c/a, and the unit-cell volume V for the $La_{1.85-x}Sr_{0.15+x}Cu_{1-x}Fe_xO_4$ $(0 \leqslant x \leqslant 1)$ samples. The lattice parameter a increases monotonously with increasing x, while c decreases. A continuous decrease in c/a can, therefore, been seen in the table. The unit-cell volume increases rapidly with doping for $x<0.5$. For $x \geqslant 0.5$, V increases very slowly, and it decreases as x approaches 1. These changes confirm that Fe substitutes on the Cu-site. The c/a ratio is generally used to characterize the Jahn–Teller distortion of the oxygen octahedron around Cu^{2+}. Obviously, Fe doping releases the Jahn–Teller distortion of the CuO_6 octahedron markedly, which should lead to changes of the transport properties.

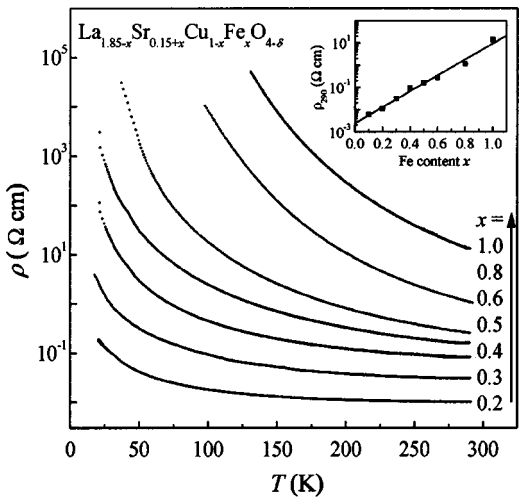

FIG. 1. The temperature dependence of the resistivity of $La_{1.85-x}Sr_{0.15+x}Cu_{1-x}Fe_xO_4$ $(0.2 \leqslant x \leqslant 1.0)$. The inset shows the room temperature resistivity (ρ_{290}) vs Fe content x.

Figure 1 shows the temperature dependence of the resistivity for $La_{1.85-x}Sr_{0.15+x}Cu_{1-x}Fe_xO_4$ at high doping levels: $x \geqslant 0.2$. One can see that all the samples show semiconducting-like behavior in the whole measured temperature range, which is in contrast to the previously studied samples with $x \leqslant 0.13$ that exhibit metal-like behavior above 200 K.[5] At high doping levels Fe causes the resistivity to increase rapidly. The room temperature resistivity (ρ_{290}) as a function of doping content x is shown in the inset of Fig. 1. An exponential increase of ρ_{290} with doping is observed, which is really different from the Zn doped La214 system.[12] For the latter, the ρ_{290} versus x curve remains linear within the range of dopant concentrations of 30%. Obviously, for Fe doping the change of ρ_{290} shown in the inset of Fig. 1 deviates from the value expected from the impurity-scattering mechanism. This deviation is likely to be related to the magnetic scattering. One knows that Fe^{3+} doped into the CuO_2 layer has an effective moment of 4.9 μ_B. The strong magnetic moment is expected to play an important role in the transport behavior. It has been noted[1,15] that the local magnetic moments in the CuO_2 plane are primarily responsible for the destruction of superconductivity and affect the temperature dependence of conductivity. Even though the Zn ion is nonmagnetic, it has been inferred that for the Zn-doped La214 system a local moment is induced at Cu sites adjacent to Zn.[16] The moment is just about 1.0 μ_B, close to that of Cu^{2+} (0.8 μ_B), indicating that a magnetic impurity-scattering mechanism may be suitable also for Zn doping.

Figure 2 shows the $\ln\rho$ versus $1/T$ curves for $La_{1.85-x}Sr_{0.15+x}Cu_{1-x}Fe_xO_4$ $(x \geqslant 0.2)$. A good linear behavior of $\ln\rho$-$1/T$ was obtained in the temperature range 150–300 K, which indicates that a thermally activated conduction mechanism dominates the transport behavior at the high temperature range. The slope of $d(\ln\rho)/d(1/T)$ (as shown in Fig. 2) increases, implying that the thermal activation energy increases with doping. This will be discussed later.

Figure 3 shows the temperature dependence of the thermoelectric power for $La_{1.85-x}Sr_{0.15+x}Cu_{1-x}Fe_xO_4$ $(0.2 \leqslant x$

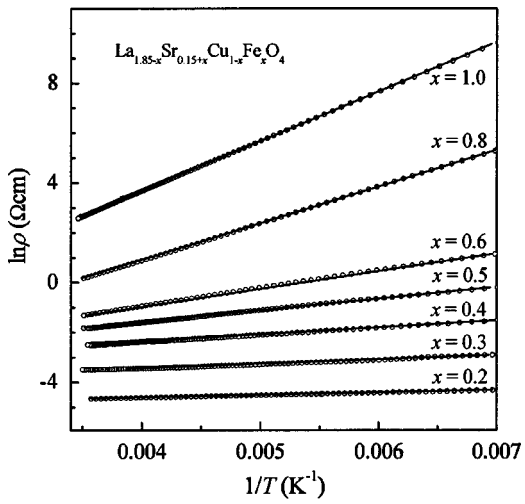

FIG. 2. Resistivity in a logarithmic scale vs $1/T$ for $La_{1.85-x}Sr_{0.15+x}Cu_{1-x}Fe_xO_4$ ($0.2 \leqslant x \leqslant 1.0$) with temperature range of 140–300 K. More than 60% points were skipped in the figure. The straight lines in the figure are linear fits at high temperatures and give the thermal activation energy ε_a^{ρ}.

$\leqslant 0.8$). The sample with $x=1.0$ has been excluded because of its deviating oxygen content and the presence of impurity phases. All the TEP values are positive, indicating hole conduction. Double doping causes the TEP to increase gradually. Every $S(T)$-T curve in Fig. 3 shows a broad peak, and the temperature (T_m) corresponding to the peak decreases with increasing x, which is in contrast to the results at low doping levels.[5]

Figure 4 shows T_m and the room temperature TEP (S_{290}) as a function of doping level x. With double doping S_{290} decreases first and reaches the lowest value at about $x=0.2$, and then begins to increase with further increase of x, while T_m shows an opposite change compared to S_{290}, as shown in Fig. 4. A characteristic of the two curves is the coincidence of the transition point at the doping level x

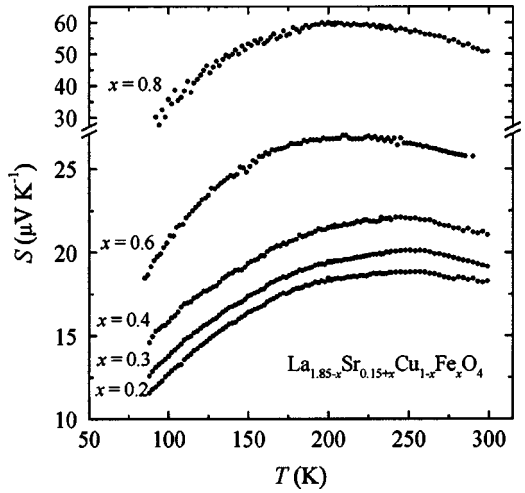

FIG. 3. The thermoelectric power as a function of temperature for $La_{1.85-x}Sr_{0.15+x}Cu_{1-x}Fe_xO_4$ ($0.2 \leqslant x \leqslant 0.8$). Lines are guides to the eyes.

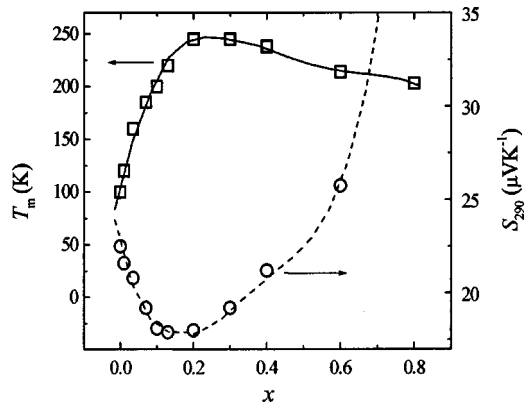

FIG. 4. T_m and S_{290} as a function of x for samples $La_{1.85-x}Sr_{0.15+x}Cu_{1-x}Fe_xO_4$.

$=0.2$, which may imply that a similar factor influences T_m and S_{290}. For high-T_c copper oxides, the temperature dependence of TEP, $S(T)$-T, shows a broad maximum below room temperature that can be characterized by a hump superposed on a weakly temperature-dependent background to give a maximum added contribution of about 15 mV/K at some characteristic temperature. Elemental doping can cause a shift of the wide peak. Many models have been proposed to explain the origin of the broad peak in the $S(T)$-T curve, such as electron–phonon interaction, the spin-fluctuation,[17] spin bag,[18] NL,[19] and resonant-valence-bond (RVB)[20] models. The first one is very successful in accounting for normal metals and alloys, but, due to the low Debye temperature, it can hardly explain the transport data of high-T_c copper oxide superconductors. For the latter, the characteristic energy replacing the Debye energy is a low-lying magnetic excitation, which means that the TEP is field-dependent. Magnetic experiments reported by R. C. Yu *et al.*[21] indicate that the TEP is independent of magnetic field up to 30 T. This result casts doubt on the magnetic models that utilize magnetic excitations as a characteristic energy. The vibronic coupling of electrons to the optical lattice vibrations proposed by Zhou *et al.*[22] can be used to account for the transport data of most high-T_c copper oxide superconductors. However, this model cannot be used to interpret the transport data involving strong spin scattering or local magnetic scattering, because it completely ignores the magnetic interaction. We have compared the transport properties of $La_{1.85-x}Sr_{0.15+x}Cu_{1-x}Fe_xO_4$ ($0 \leqslant x \leqslant 0.13$) with those of $La_{1.85-x}Sr_{0.15+x}Cu_{1-x}Ga_xO_4$ ($0 \leqslant x \leqslant 0.2$) and found that Fe doping leads to an upwards shift of T_m from 100 to 200 K as x increases from 0 to 0.13, while for the Ga doped system T_m is nearly unchanged.[5] Similar results have also been obtained in $Bi_2Sr_{2-x}CuO_6$[23] and $Bi_2Sr_2Ca_{1-x}Y_xCu_2O_y$.[24] These suggest that the localized magnetic scattering influence T_m markedly.

To examine the possibility of polaron transport in $La_{1.85-x}Sr_{0.15+x}Cu_{1-x}Fe_xO_4$, we compare the thermal activation energy derived from resistivity with that from TEP. For a thermal activated conduction process, the resistivity and TEP should show the following temperature dependence, respectively:

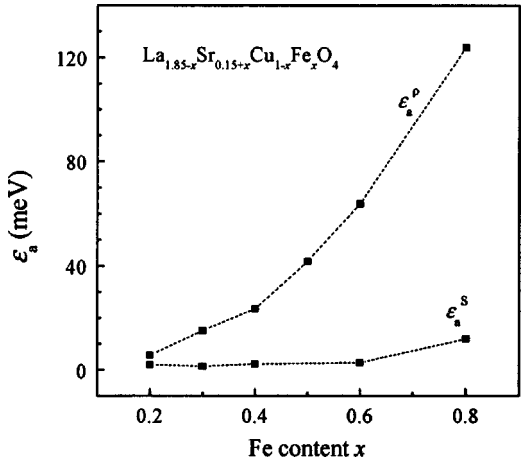

FIG. 5. Thermal activation energy (ε_a^ρ and ε_a^S) derived from the resistivity and TEP vs the Fe content x for $La_{1.85-x}Sr_{0.15+x}Cu_{1-x}Fe_xO_4$.

$$\rho(T)=\rho_0\exp(\varepsilon_a/kT) \quad \text{and} \quad S(T)=\pm(k/e)(\varepsilon_a/kT+A).$$

Where the + and − sign hold for hole-type and electron-type of conduction, and the constant A is determined by the energy dependence of the scattering time.[25] Here, we use ε_a^ρ and ε_a^S to denote the activation energies derived from resistivity and TEP, respectively. The results are shown in Fig. 5. While ε_a^ρ increases rapidly with double doping, ε_a^S is essentially constant, except for $x=0.8$. Here it is noteworthy that ε_a^ρ is very close to ε_a^S for the $x=0.2$ sample. With further increase of x ε_a^ρ is systematically larger than ε_a^S, and the difference between ε_a^ρ and ε_a^S, $\varepsilon_a^\rho-\varepsilon_a^S$, enhances progressively with increasing x to reach a maximum of 111.9 meV at $x=0.8$. The great discrepancy can be understood in terms of a small magnetic polaron model. So called small magnetic polarons are the self-localized states induced by the magnetic coupling between magnetic ions and hole spins.[26–28] From the small magnetic polaron model, it can be deduced that the polaron formation energy ε_p is twice as large as the difference between ε_a^ρ and ε_a^S, i.e., for the sample with $x=0.8$ the polaron formation energy is $\varepsilon_p=2(\varepsilon_a^\rho-\varepsilon_a^S)=223.8$ meV. This value is close to 204, 221, and 220 meV observed in $La_{2/3}Ca_{1/3}MnO_3$,[29] $La_{1.05}Sr_{0.95}Cu_{0.2}Co_{0.8}O_y$,[6] and $La_{1.85}Sr_{0.15}NiO_4$,[27] respectively, which suggests that small magnetic polaron conduction dominates the transport behavior at high doping level.

Figure 6 shows the polaron formation energy (ε_p) as a function of doping level x. For comparison, the results calculated from the $La_{1.85}Sr_{0.15}Cu_{1-x}Ni_xO_4$ and $La_{1.85-x}Sr_{0.15+x}Cu_{1-x}Co_xO_4$ systems are also given in the figure. A common characteristic for the three systems is that all the formation energies increase with doping and the values are higher than 200 meV at high doping levels. For the Co and Ni doped systems, $\varepsilon_p(x)$ shows a similar change, namely that ε_p increases rapidly at small x and then more slowly. For the Co doped system, it even decreases slightly for $x\geqslant 0.8$. This is in contrast to the behavior of the Fe doped system, where a steady increase of $\varepsilon_p(x)$ is observed. The

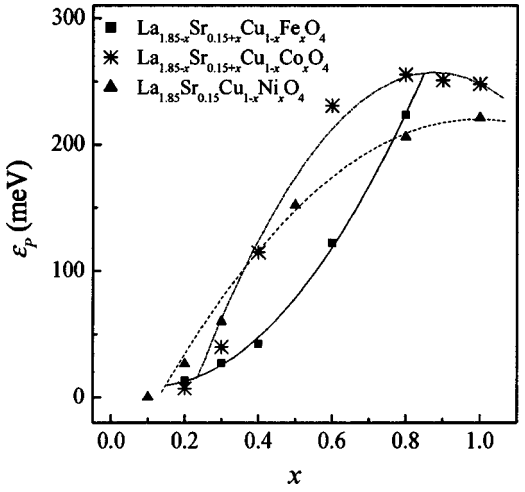

FIG. 6. Polaron formation energy ε_p vs dopant content x for $La_{1.85-x}Sr_{0.15+x}Cu_{1-x}M_xO_4$ (M=Fe, Co, and Ni).

different behaviors are suggested to be related to the change of the spin correlations, which will be discussed later. It has been suggested that the formation energy of polarons is closely related to the size of polaron. The polaron generally tends to expand with the reduction of formation energy. For example, for $La_{1.85}Sr_{0.15}CuO_{4+\delta}$ the ε_p determined from optical conducting measurements is 60 meV, which is only a quarter of the ε_p in $La_{1.85}Sr_{0.15}NiO_4$.[27] However, the polaron size of the former is almost 10 times larger than the latter. Obviously, Fe, Co, and Ni doping favor the formation and development of small polarons. From the tendency in Fig. 5 it is speculated that ε_p for the Fe doped samples with x close to 1.0 should be bigger than that for the Co and Ni doped samples.

Figure 7 shows the ESR signals at 100 K for the samples of the $La_{1.85-x}Sr_{0.15+x}Cu_{1-x}Fe_xO_4$ system. The g factor corresponding to the ESR lines is ~2.0, indicating the predominance of Fe^{3+} spins. It is found that the ESR signal intensifies gradually with increasing Fe content and reaches a

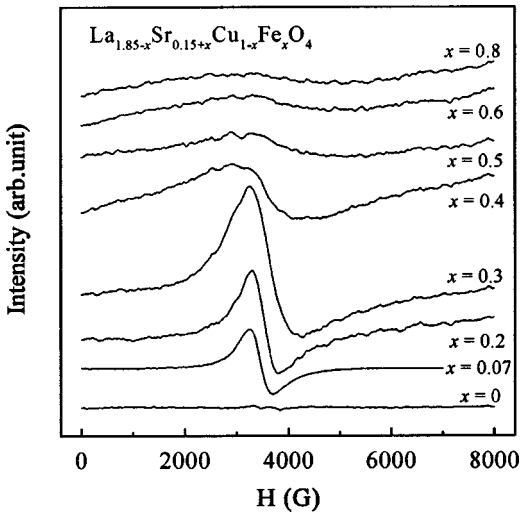

FIG. 7. ESR spectra of $La_{1.85-x}Sr_{0.15+x}Cu_{1-x}Fe_xO_4$ ($0\leqslant x\leqslant 0.8$) measured at 100 K.

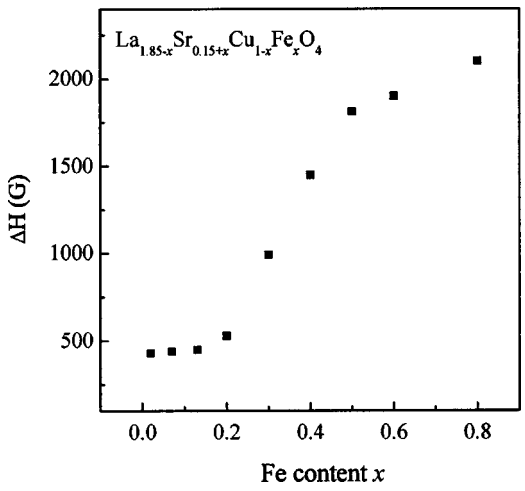

FIG. 8. ESR linewidth as a function of x for $La_{1.85-x}Sr_{0.15+x}Cu_{1-x}Fe_xO_4$ ($0 \leqslant x \leqslant 0.8$).

maximum intensity at $x=0.3$, and then weakens with further increase of x. The ESR linewidth, ΔH, increases continuously with doping, as shown in Fig. 8. Replacing Cu^{2+} with Fe^{3+} in the CuO_2 plane destroys the original Cu–O–Cu spin correlation. Fe^{3+} possesses a half full $3d$ electron shell ($3d^5$) in La214 with a spin state of $S=5/2$, which is quite different from that of Cu^{2+}. The strong magnetic moment of Fe^{3+} weakens the correlation with the nearby Cu^{2+}. Localized Fe^{3+} spins are formed in the compound, and a marked ESR signal is detected. With increasing x the number of localized Fe^{3+} spins increases, and so does the intensity of ESR signal. For $x>0.2$, it is possible that part of the Fe^{3+} ions correlate and new spin correlations, Fe^{3+}–O–Fe^{3+}, begin to form. This causes the Fe^{3+} spin–spin relaxation time to increase. The previous study[12] on weakly Fe-doped La214 show that for $x \geqslant 0.1$ the linewidth at 100 K is mainly given by the spin–spin relaxation rate. Based on this analysis, one can well understand the rapid increase of ΔH with doping for $x \geqslant 0.2$, as well as the decrease in intensity of the ESR signals at high doping level shown in Figs. 7 and 8.

Spin (magnetic) scattering could markedly influence the NS transport properties, as was reported previously.[24,30] The change of localized magnetic scattering by Fe^{3+} dominates the change of T_m in Fig. 3. That is, at low doping level the gradual increase of localized magnetic scattering with Fe doping causes T_m to increase from 110 to 248 K. At high doping level, the formation of Fe–O–Fe spin correlations causes delocalization of the Fe^{3+} spins and the effect of localized magnetic scattering on T_m decreases. As a result, the broad peak shifts down to low temperature (see Fig. 4).

Let us now turn to the different behavior of $\varepsilon_p(x)$ as a result of Fe, Co, and Ni doping shown in Fig. 6. Compared to Fe^{3+}, Co^{3+}, and Ni^{2+} possess low magnetic moments (1.0 and 0.7 μ_B, respectively) in the La214 system,[1] close to that of Cu^{2+}. Co can exist in the La214 system with different spin states at different temperatures (low spin state, middle spin state and high spin state).[31,32] As they replace Cu in the CuO_2 plane, the Ni and Co spins could correlate with the Cu spins. Our ESR experiment results show that no ESR signals can be detected in samples of $La_{1.85-x}Sr_{0.15+x}Cu_{1-x}Co_xO_4$ ($0 \leqslant x \leqslant 1$) and $La_{1.85}Sr_{0.15}Cu_{1-x}Ni_xO_4$ ($x \leqslant 0.5$).[33] This suggests that Co and Ni spins do not localize. Due to the strong localization of Fe^{3+} at low doping level, polarons are hardly formed and have little influence on the transport behavior, which is quite different from that in the Co and Ni doped systems. Only at high doping levels, the polaron transport may play an important role in the conduction of Fe doped La214.

CONCLUSION

The structure, transport properties and spin correlation of double-doped $La_{1.85-x}Sr_{0.15+x}Cu_{1-x}Fe_xO_4$ were studied carefully. Double doping leads to an increase of the lattice parameters a in the whole doping range and c is decreasing. By analyzing the discrepancy of the thermal activation energy derived from the resistivity and TEP, it is found that the transport mechanism at high doping level can be understood in terms of polaron conduction. The ESR result suggests that the Fe^{3+} spins change from localization to delocalization as x changes from low doping level to high doping level. A close relation between localized spin scattering and T_m is also proposed.

ACKNOWLEDGMENTS

This work was supported by the National Natural Science Foundation of China (No. 0074057) and the Danish Technical Research Council under the Framework Program on Superconductivity.

*Electronic address: xugj@hotmail.com

[1] Gang Xiao, Marta Z. Cieplak, J. Q. Xiao, and C. L. Chien, Phys. Rev. B **42**, 8752 (1990).
[2] N. Ishikawa, N. Kuroda, H. Ikeda, and Yoshizaki, Physica C **203**, 284 (1992).
[3] D. Vaknin, S. K. Sinha, D. E. Moncton, D. C. Johnston, J. M. Newsam, C. R. Safinya, and H. E. King, Phys. Rev. Lett. **58**, 2802 (1987).
[4] Xu Gaojie, Mao Zhiqiang, Tian Mingliang, Wang Yu, and Zhang Yuheng, J. Supercond. **10**, 13 (1997).
[5] Xu Gaojie, Pu Qirong, Ding Zejun, and Zhang Yuheng, J. Phys.: Condens. Matter **12**, 8231 (2000).
[6] Xu Gaojie, Mao Zhiqiang, Jin Hao, Yan Hongjie, Wang Bin, and Zhang Yuheng, Phys. Rev. B **59**, 12 090 (1999).
[7] B. I. Kochelaev, L. Kan, B. Elschner, and S. Elschner, Phys. Rev. B **49**, 13 106 (1994).
[8] Xu Gaojie, Mao Zhiqiang, Jin Hao, Yan Hongjie, Tian Mingliang, and Zhang Yuheng, Physica C **314**, 263 (1999).
[9] Xu Gaojie, Mao Zhiqiang, Yan Hongjie, Jin Hao, Tian Mingliang, Wu Yicheng, and Zhang Yuheng, Supercond. Sci. Technol. **12**, 417 (1999).
[10] J. Takeda, T. Nishikawa and M. Sato, Physica C **231**, 293 (1994).
[11] Xu Gaojie, Mao Zhiqiang, Yan Hongjie, Jin Hao, Tian Mingliang, and Zhang Yuheng, J. Supercond. **12**, 417 (1999).

[12] Marta Z. Cieplak, A. Sienkiewicz, F. Mila, S. Guha, Gang Xiano, J. Q. Xiao, and C. L. Chien, Phys. Rev. B **48**, 4019 (1993).
[13] Mao Zhiqiang, Xu Gaojie, Yan Hongjie, Wang Bin, Qiu Xueyin, and Zhang Yuheng, Phys. Rev. B **58**, 15 116 (1998).
[14] Pu Qirong, Xu Gaojie, Zhang Zengmin, and Ding Zejun, Physica C **370**, 163 (2002).
[15] Marta Z. Cieplak, S. Guha, H. Kojima, P. Lindenfeld, Gang Xiao, J. Q. Xiao, and C. L. Chien, Phys. Rev. B **46**, 5536 (1992).
[16] A. V. Mahajan, H. Alloul, G. Collin, and J. F. Marucco, Phys. Rev. Lett. **72**, 3100 (1994).
[17] A. J. Millis, H. Monien, and D. Pines, Phys. Rev. B **42**, 167 (1990).
[18] J. R. Schrieffer, X. G. Wen, and S. C. Zhang, Phys. Rev. Lett. **60**, 944 (1988); Phys. Rev. B **39**, 11 663 (1989).
[19] N. Nagaosa and P. A. Lee, Phys. Rev. Lett. **64**, 2450 (1990).
[20] P. W. Anderson, Science **215**, 1196 (1987).
[21] R. C. Yu, M. J. Naughton, X. Yan, and P. M. Chaikin, Phys. Rev. B **37**, 7963 (1988).
[22] J. S. Zhou and J. B. Goodenough, Phys. Rev. B **51**, 3104 (1995).
[23] Xu Gaojie, Mao Zhiqiang, Yan Hongjie, and Zhang Yuheng, J. Phys.: Condens. Matter **10**, 8843 (1998).
[24] Xu Gaojie, Pu Qirong, Ding Zejun, Yang Li, and Zhang Yuheng, Phys. Rev. B **62**, 9172 (2000).
[25] N. F. Mott and E. A. Davis, *Electronic Processes in Non-crystalline Materials* (Oxford, London, 1971).
[26] I. Anisimov, M. A. Korotin, J. Zoanen, and O. K. Andersen, Phys. Rev. Lett. **68**, 345 (1992).
[27] X.-X. Bi and P. C. Eklund, Phys. Rev. Lett. **70**, 2625 (1993).
[28] S.-W. Cheong, H. Y. Hwang, C. H. Chen, B. Batlogg, L. W. Rupp, Jr., and S. A. Carter, Phys. Rev. B **49**, 7088 (1994).
[29] R. Muhlstroh and H. G. Reik, Phys. Rev. **162**, 703 (1967).
[30] Xu Gaojie, Mao Zhiqiang, Tian Mingliang, Wu Wenbin, and Zhang Yuheng, J. Supercond. **10**, 555 (1997).
[31] M. A. Korotin, S. Y. Ezhov, I. V. Solovyev, V. I. Anisimov, D. I. Khomskii, and G. A. Sawatzky, Phys. Rev. B **54**, 5309 (1996).
[32] Y. Moritomo, K. Higashi, Matsuda, and A. Nakamura, Phys. Rev. B **55**, R14 725 (1997).
[33] G. J. Xu and Z. Q. Mao (unpublished).